J|A|C|S ARTICLES

Published on Web 08/31/2010

NMR-Spectroscopic and Solid-State Investigations of Cometal-Free Asymmetric Conjugate Addition: A Dinuclear Paracyclophaneimine Zinc Methyl Complex

S. Ay,[†] R. E. Ziegert,[†] H. Zhang,[‡] M. Nieger,[§] K. Rissanen,[□] K. Fink,[¶] A. Kubas,[¶] R. M. Gschwind,*[,‡] and S. Bräse*[,†]

Institute of Organic Chemistry, Karlsruhe Institute of Technology (KIT), Fritz-Haber-Weg 6, D-76131 Karlsruhe, Germany, Institute of Organic Chemistry, University of Regensburg, D-93040 Regensburg, Germany; Laboratory of Inorganic Chemistry, University of Helsinki, P.O. Box 55 (A.I. Virtasen aukio 1), FIN-00014 University of Helsinki, Finland; Laboratory of Organic Chemistry, University of Jyväskylä, P.O. Box 35, FIN-40014 University of Jyväskylä, Finland; Institute of Nanotechnology (INT), Karlsruhe Institute of Technology (KIT), Hermann-von-Helmholtz-Platz 1, D-76344 Eggenstein-Leopoldshafen, Germany

Received April 23, 2010; E-mail: ruth.gschwind@chemie.uni-regensburg.de; braese@kit.edu

Abstract: We present herein the first indications for dimeric structures in cometal-free asymmetric conjugate addition reactions of dialkylzinc reagents with aldehydes. These are revealed by nonlinear effect (NLE) studies. A monomer−dimer equilibrium can be assumed which explains the increase of the ee value in the product over time. Also, DOSY NMR spectroscopic measurements indicate the existence of the catalyst as $[LZnEt]_n$ complexes in solution. Additionally, the first X-ray structure of a zinc complex with a [2.2]paracyclophane ligand was determined. The structures of the zinc complexes are supported by DFT calculations of monomeric and dimeric species.

1. Introduction

The asymmetric conjugate addition (ACA) reaction is one of the most powerful C−C bond-forming reactions in modern organic chemistry.[1] Beside existing copper- or rhodium-catalyzed additions of dialkylzinc reagents, our group showed that [2.2]paracyclophane-based *N*,*O*-ligands allow an efficient zinc-catalyzed alternative, which occurs without additional metal salts (cometals are copper or rhodium in addition to the organometallic reagents such as dialkylzinc or Grignard reagents).[2] Moreover, this system is compatible with enals, which—due to the high electrophilicity of the aldehyde group—often cause chemoselectivity problems with other catalytic systems. Although efficient systems were developed to react Grignard[3] and aluminum[4] reagents in 1,4-addition reactions, zinc reagents are still very attractive due to their high tolerance toward a wide range of functional groups. Typically, organo−zinc compounds react with electrophiles in 1,2-addition reactions.[5] The postulated mechanism is investigated experimentally and theoretically.[6] In contrast, no mechanistic investigations have been made so far to explain the unexpected 1,4-selectivity of our [2.2]paracyclophane-based system reacting dialkylzinc reagents with enals.

Herein we present the first mechanistic insights in this direction. Besides nonlinear effect (NLE) studies, zinc catalyst intermediates of the cometal-free ACA were studied by NMR techniques in solution. Furthermore, we present the first X-ray structure of a zinc−[2.2]paracyclophane complex. Finally, DFT calculations supported our findings.

2. Results and Discussion

Recently, we were able to optimize the [2.2]paracyclophane ligand structure for conjugate addition reactions of diethylzinc

[†] Organic Chemistry, KIT.
[‡] University of Regensburg.
[§] Laboratory of Inorganic Chemistry, University of Helsinki.
[□] Laboratory of Organic Chemistry, University of Jyväskylä.
[¶] INT, KIT.

(1) (a) López, F.; Feringa, B. L. In *Asymmetric Synthesis: The Essentials*; Christmann, M., Bräse, S., Eds.; Wiley-VCH: Weinheim, 2008, pp 78−83. (b) Alexakis, A.; Benhaim, C. *Eur. J. Org. Chem.* **2002**, 3221–3236. (c) Krause, N.; Hoffmann-Röder, A. *Synthesis* **2001**, 171–196. (d) Perlmutter, P. *Conjugate Addition Reactions in Organic Synthesis*, Tetrahedron Organic Chemistry Series, Vol. 9; Pergamon: Oxford, 1992.

(2) Bräse, S.; Höfener, S. *Angew. Chem.* **2005**, *117*, 8091–8093. *Angew. Chem., Int. Ed.* **2005**, *44*, 4879−7881.

(3) (a) Bos, P. H.; Minnaard, A. J.; Feringa, B. L. *Org. Lett.* **2008**, *10*, 4219–4222. (b) Harutyunyan, S. R.; den Hartog, T.; Geurts, K.; Minnaard, A. J.; Feringa, B. L. *Chem. Rev.* **2008**, *108*, 2824–2852. (c) López, F.; Minnaard, A.; Feringa, B. L. *Acc. Chem. Res.* **2007**, *40*, 179–188.

(4) (a) Hawner, C.; Li, K.; Cirriez, V.; Alexakis, A. *Angew. Chem.* **2008**, *120*, 8334–8337. Angew. Chem., Int. Ed. 2008, *47*, 8211−8214. (b) d'Augustin, M.; Alexakis, A. *Tetrahedron Lett.* **2007**, *48*, 7408–7412. (c) Alexakis, A.; Albrow, V.; Biswas, K.; d'Augustin, M.; Prieto, O.; Woodward, S. *Chem. Commun.* **2005**, *22*, 2843–2845.

(5) Review about substrates with carbonyl moieties: Pu, L.; Yu, H.-B. *Chem. Rev.* **2001**, *101*, 757–824. High enantioselectivities have been obtained with *N*,*N*-(dimethylamino)isoborneol (DAIB) as ligand and aldehydes as substrates Kitamura, M.; Okada, S.; Suga, S.; Noyori, R. *J. Am. Chem. Soc.* **1989**, *111*, 4028–4036.

(6) (a) Yamakawa, M.; Noyori, R. *J. Am. Chem. Soc.* **1995**, *117*, 6327–6335. (b) Yamakawa, M.; Noyori, R. *Organometallics* **1999**, *18*, 128–133. (c) Goldfuss, B.; Houk, K. N. *J. Org. Chem.* **1998**, *63*, 8998–9006. (d) Goldfuss, B.; Steigelmann, M.; Khan, S. I.; Houk, K. N. *J. Org. Chem.* **2000**, *65*, 77–82. (e) Rasmussen, T.; Norrby, P.-O. *J. Am. Chem. Soc.* **2001**, *123*, 2464–2465.

Scheme 1. ACA of Diethylzinc with Cinnamaldehyde Utilizing [2.2]Paracyclophane Ligands[a]

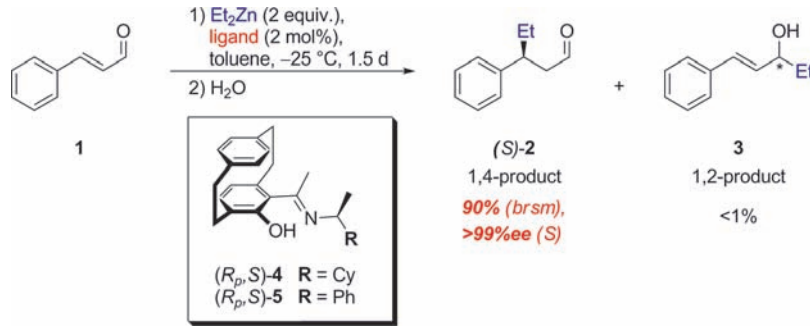

[a] brsm = based on recovered starting material.

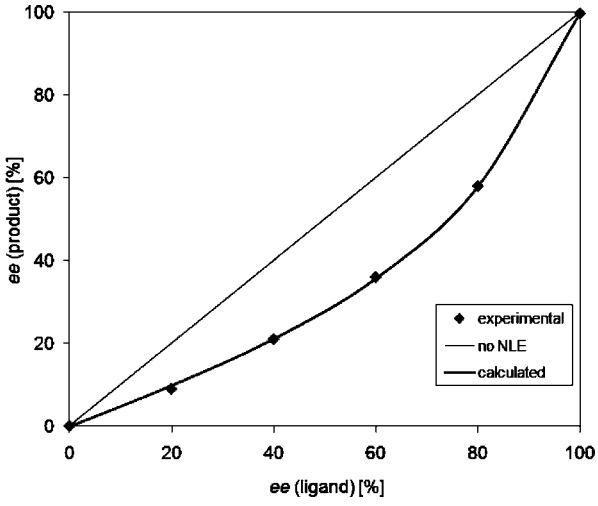

Figure 1. Observed and predicted negative NLE for the 1,4-addition reaction using (R_p,S)-**4**/(S_p,R)-**4** (0.01 M). The calculated curve is based on parameters found by fitting of the experimental values (ee_{max} = 99%): see SI.

to cinnamaldehyde.[7] Herein, the corresponding ligand **4** was used for NLE-investigations,[8] which proved to be a valuable tool for mechanistic investigations. The ligand (R_p,S)-**4** was used in enantiopurities ranging from 0% ee to >99% ee with the reaction conditions given in Scheme 1. As depicted in Figure 1, a significant *negative* NLE was observed. For the time dependency of the ee, see Supporting Information (SI).

The experimental values correlate very well with a fitted curve calculated by assuming stable homo- or heterodimers as indicated in Figure 2 (L^R and L^S are enantiomers; for mathematical models used, see SI). This is an indication for a favored formation of dimeric species. Interestingly, ligand (R_p,S)-**4** delivers also a negative NLE in 1,2-addition reactions of dialkylzinc reagents to aldehydes.[9]

In the course of our NLE studies, we also compared diastereomers (R_p,S)-**4** and (S_p,S)-**4**. The initially used enantiopure [2.2]paracyclophane ligands are obtained by chromatographic separation of the corresponding diastereomers.[10] If one diastereomer generates a catalyst which is significantly more active, a tedious chromatographic purification step might be avoided.[11] Ligand (R_p,S)-**4** was mixed with its diastereomer (S_p,S)-**4** in different de's. The results of the NLE study are shown in Figure 3. As for the different mixtures of enantiomers (Figure 1), a clear *negative* NLE is observed. The experimental values correlate again very well with a calculated fitted curve (see SI), see also Figure 2 (L^R and L^S are diastereomers). Both diastereomers deliver compound **2** in >99% ee. Ligand (R_p,S)-**4** leads to (S)-**2**, whereas (S_p,S)-**4** gives (R)-**2**. In the case of an equimolar mixture of both diastereomers, **2** is obtained in −36% ee due to a higher catalytic activity of the generated zinc catalyst with the (S_p,S)-**4** ligand. The slight difference between the experimental values and the fitted curve in comparison to Figure 1 indicates complex interactions between the diastereomeric ligands (*vide infra*).

Considering the observed NLE—besides the different activities of diastereomeric complexes of (R_p,S)-**4** and (S_p,S)-**4**—the potential formation of dimers has to be taken into account. As the NLE is negative, homodimers are likely to be more stable than the corresponding heterodimers (see section with calculated values).[9] Similar effects have been observed by Noyori using diastereomeric DAIB ligands.[12] In our case, however, the specific curve progression indicates a more complex aggregation level, which might be caused by contributions of $[LZnEt]_n$ oligomers as indicated by NMR measurements (see below).[13] Taking all considerations established so far into account, a $(ML)_2$-system is likely to exist.

In order to study the catalytically active species in more detail, NMR spectroscopic measurements were carried out. For these NMR studies of the zinc complex structure in solution, the phenyl-substituted ligand **5** was chosen (Scheme 1). This ligand allows observing reliably the formation of ethylzinc complexes due to fewer signals in the aliphatic region of the ^{1}H NMR spectrum.

(7) Ay, S.; Nieger, M.; Bräse, S. *Chem.—Eur. J.* **2008**, *14*, 11539–11556.
(8) NLE = non linear effect: (a) Girard, C.; Kagan, H. B. *Angew. Chem.* **1998**, *110*, 3088–3127. *Angew. Chem., Int. Ed.* **1998**, *37*, 2923−2959. (b) Kagan, H. B. *Adv. Synth. Catal.* **2001**, *343*, 227–233. (c) Satyanarayana, T.; Abraham, S.; Kagan, H. B. *Angew. Chem.* **2009**, *121*, 464–503. *Angew. Chem., Int. Ed.* **2009**, *48*, 456−494. (d) For a recent example of a (−)-NLE showing that the homodimer is more stable than the heterodimer: Kina, A.; Iwamura, H.; Hayashi, T. *J. Am. Chem. Soc.* **2006**, *128*, 3904–3905.
(9) Lauterwasser, F.; Vanderheiden, S.; Bräse, S. *Adv. Synth. Catal.* **2006**, *348*, 443–448.
(10) Bräse, S.; Dahmen, S.; Höfener, S.; Lauterwasser, F.; Kreis, M.; Ziegert, R. E. *Synlett* **2004**, 2647–2669.
(11) Bolm, C.; Muniz, K.; Hildebrand, J. P. *Org. Lett.* **1999**, *1*, 491–493.
(12) Kitamura, M.; Suga, S.; Niwa, M.; Noyori, R. *J. Am. Chem. Soc.* **1995**, *117*, 4832–4842.
(13) Similar curves (using *enantiomeric* ligands) were obtained in Ti-catalyzed asymmetric oxidations of sulfides (Kagan[13a]) and in Cu-catalyzed ACA of Grignard reagents to enones (Pfaltz and Zhou[13b]). But also in these cases the exact structure of the participating species remained unknown due to complex equilibria: (a) Guillaneux, D.; Zhao, S.-H.; Samuel, O.; Rainford, D.; Kagan, H. B. *J. Am. Chem. Soc.* **1994**, *116*, 9430–9439. (b) Zhou, Q.-L.; Pfaltz, A. *Tetrahedron* **1994**, *50*, 4467–4478.

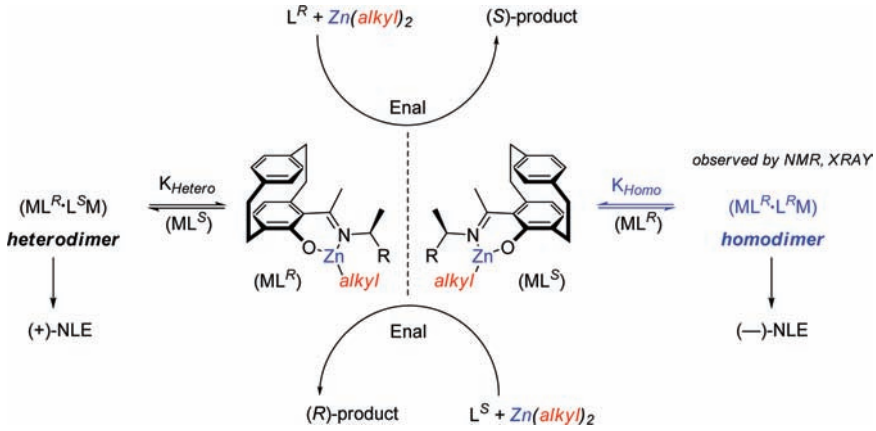

Figure 2. Model for the cometal-free ACA. L^R and L^S are either enantiomers or diastereomers.

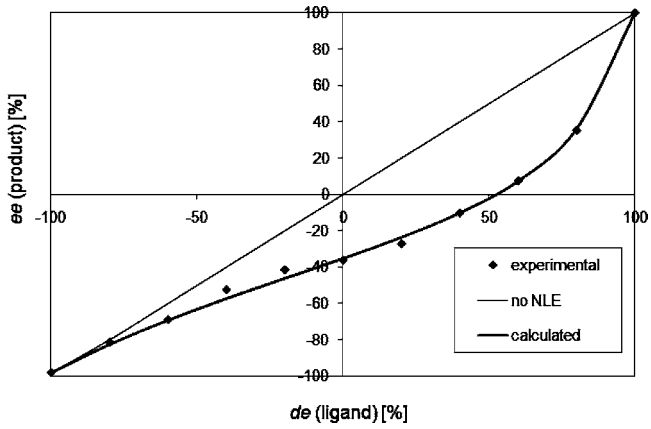

Figure 3. Activity investigation of mixtures of diastereomeric catalysts (R_p,*S*)-**4** (corresponding to −100% de) and (S_p,*S*)-**4** (corresponding to +100% de). The calculated curve is based on parameters found by fitting of the experimental values: see SI.

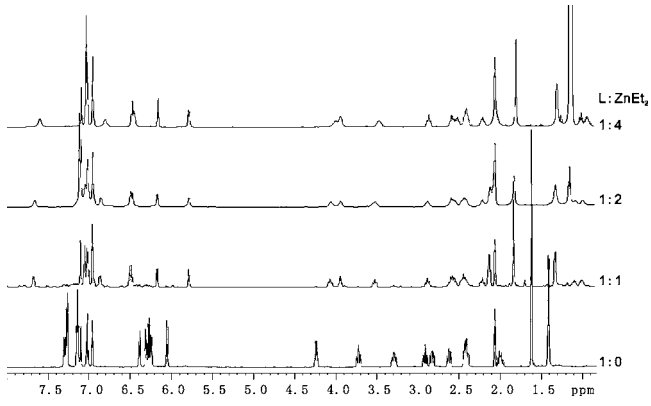

Figure 4. ^{1}H NMR spectra of (R_p,*S*)-**5** and diethylzinc in different ratios (toluene-[D_8] at 240 K).

First, ^{1}H NMR spectra of the ligand and diethylzinc at different ratios in toluene-[D_8] were measured to identify the stoichiometry of the complex (see Figure 4).

At a 1:1 ratio of (R_p,*S*)-**5** and diethylzinc, the signals of the free ligand completely disappeared, and a new set of signals with different chemical shifts and broader line widths is observed. The complete ^{1}H and ^{13}C chemical shift assignment of the zinc complex with the signals of the metal-bound ethyl substituent (at 2.14 ppm (CH_3) and 1.10 and 1.01 ppm (diastereotopic CH_2), see SI for further details) indicates the

Table 1. Diffusion Coefficients *D* (10^{-10} m^2 s^{-1}) and Volumes *V* (Å^3) of the Free Ligand and of the Zinc Complex Derived from a 1:1 Ratio (**5**:Et_2Zn)[a]

entry	temperature [K]	D_{ligand}	V_{ligand}	$D_{complex}$	$V_{complex}$	n[b]
1	270	2.13	479	1.45	1506	2.8
2	260	2.11	494	1.39	1710	3.1
3	250	2.08	511	1.36	1856	3.4
4	240	2.09	509	1.32	1992	3.7
5	230	2.10	498	1.29	2136	3.9

[a] Measured as 0.02 M solutions in toluene-[D_8]. [b] The multiple *n* is based on the formula $[ZnEtL]_n$.

successful formation of a zinc complex with a 1:1 stoichiometry. At ratios higher than 1:1, the signal pattern of the zinc complex does not change significantly, and additional signals of the free uncomplexed diethylzinc appear at 1.13 and 0.06 ppm. It is noteworthy that the line widths of the signals increase slightly. This line broadening can be most probably attributed to an exchange process of the ethyl substituent between the complex and the uncomplexed diethylzinc, which is observed in NOESY spectra (see SI). As a result, the NMR spectra indicate that exclusively zinc complexes with the stoichiometry $(ZnEtL)_n$ are formed in solution even in the presence of an excess of Et_2Zn.

Diffusion-ordered ^{1}H NMR experiments (DOSY) have been successfully applied to obtain information about organometallic aggregates and complexes in solution, providing a realistic picture of microscopic dynamics.[14] Therefore, DOSY experiments were chosen to investigate the size of the complex $(ZnEtL)_n$, its aggregation level *n* and the temperature-dependence of the aggregation. The diffusion coefficients of the free ligand and of the complex were measured in a temperature zone between 230 and 270 K, which lies in the synthetically relevant area. For intensity reasons the concentration of the samples was chosen to be double as high (0.02 M) as for the NLE studies (0.01 M) to obtain reliable diffusion coefficients. The resulting temperature- and viscosity-corrected diffusion coefficients are summarized in Table 1.

For the indicated temperatures, the diffusion coefficient of (R_p,*S*)-**5** (D_{ligand}) remains constant within the experimental error of ±3%. The corresponding volumes indicate monomeric ligand structures. For a monomeric zinc complex (ZnEtL) the diffusion

(14) (a) Henze, W.; Gärtner, T.; Gschwind, R. M. *J. Am. Chem. Soc.* **2008**, *130*, 13718–13726. (b) Schober, K.; Zhang, H.; Gschwind, R. M. *J. Am. Chem. Soc.* **2008**, *130*, 12310–12317. (c) Zhang, H.; Gschwind, R. M. *Angew. Chem.* **2006**, *118*, 6540–6544. *Angew. Chem., Int. Ed.* **2006**, *45*, 6391–6394.

coefficients would be similar to that of the free ligand, since the additional volume of EtZn is relatively small. Surprisingly, the diffusion coefficients of the 1:1 complex are significantly smaller and show a slight temperature dependence, which indicates aggregation of the complex in solution. On the basis of the complex stoichiometry $[ZnEtL]_n$ (see above) and hard sphere increments, an aggregation level of $n = 2.8$ was calculated for 270 K, which increases at lower temperatures (up to $n = 3.9$ at 230 K, see Table 1). In accordance with the results of the ^{1}H NMR spectra (Figure 4) also further DOSY measurements show that increased amounts of Et_2Zn up to 4:1 (Et_2Zn to ligand) do not affect the structure or aggregation of the complexes. The excess of Et_2Zn causes only exchange peaks between the free and bound EtZn in EXSY spectra, but the diffusion coefficients of the resulting complexes are nearly identical to those of the 1:1 samples (see SI). The presented data show that despite the bulky [2.2]paracyclophane ligand the zinc complex of **5** is aggregated and not monomeric in toluene. The missing self-aggregation of the free ligand compared to the $[ZnEtL]_n$ complex indicates a Zn-mediated aggregation mechanism in solution. The nearly linear slope of the aggregation level *n* with decreasing temperature hints at an aggregation structure with sticky ends.[15] Another explanation would be a very flat hyperpotential surface of the dimeric, trimeric, and tetrameric aggregates for the complexes of (R_p,*S*)-**5**. In contrast, for equilibria between strongly defined aggregates, plateau values of the diffusion coefficients are often observed.[16]

As a result the DOSY investigations show, despite the bulky paracyclophane ligand (R_p,*S*)-**5**, a distinct tendency for the aggregation of the complex $(ZnEt\cdot\mathbf{5})_n$ in toluene with aggregation numbers between 2.8 and 3.9. To this increased aggregation of (ZnEt·**5**) compared to the NLE studies with (ZnEt·**4**) two spectroscopically necessary deviations in the experimental setup may contribute. First, higher concentrations, as used in the NMR compared to the NLE studies, are well-known to induce a higher degree of aggregation in solution.[17] Second, the aggregation level of paracyclophane zinc complexes might be sensitive to small changes in the ligand structure as similarly found in phosphoramidite copper complexes.[18] Thus, the lower sterical hindrance and the reduced amount of entropic degrees of freedom of the phenyl ring in **5** (necessary for the chemical shift dispersion in the NMR studies) compared to the cyclohexyl ring in **4** (used in the NLE studies) may additionally cause a slightly higher aggregation in solution. Thus, in agreement with each other, NMR and NLE studies show both aggregated $[LZnEt]_n$ complexes in solution with the actual aggregation level *n* dependent on concentration and ligand structure.

The observation of one set of NMR signals at all temperatures investigated shows that in solution the paracyclophane zinc complexes exist as symmetrically aggregated species with

Scheme 2. (a) Possible Conformations of the Zinc Complex ZnEt·**5**; (b) NOE Pattern of a 1:1 Complex of (R_p,*S*)-**5** and Diethylzinc Derived from a NOESY Spectrum at 260 K[a]

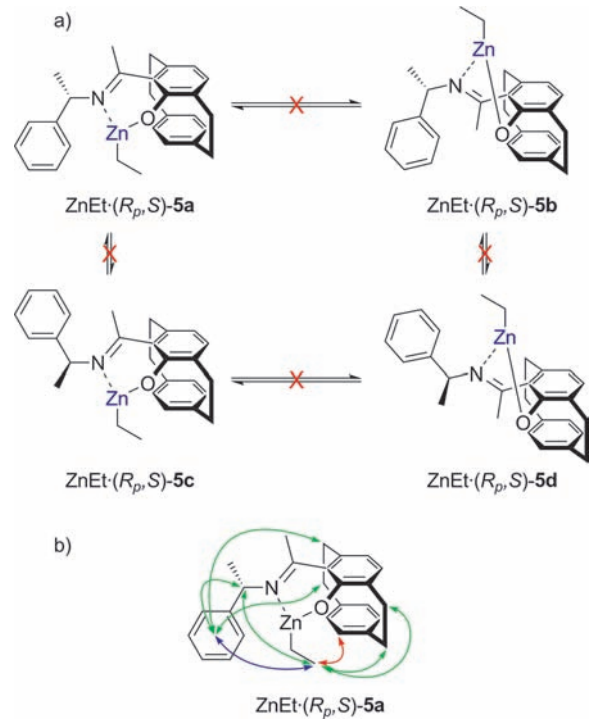

[a] The color of the arrows corresponds to the intensity of the cross peaks (red: very strong, blue: strong, green: weak).

(ZnEtL) units. Other complexes can be excluded. In principle four possible conformations of these monomeric ZnEtL units with respect to the position of the zinc atom and the phenylethyl side chain are likely to exist (Scheme 2a). The zinc atom looks either downward and is pushed from the coordinating imine-nitrogen into the paracyclophane half-space, giving conformer ZnEt·(R_p,*S*)-**5a**, or it looks up. In this case, it is above the paracyclophane scaffold leading to conformer ZnEt·(R_p,*S*)-**5b**. In the other two conformations the phenylethyl-moiety is flipped away from the paracyclophane half-space (structures ZnEt·(R_p,*S*)-**5c** and ZnEt·(R_p,*S*)-**5d**). An interconversion of the four conformations at the considered temperature range is improbable because of the steric hindrance. This is also experimentally confirmed by a series of temperature-dependent ^{1}H NMR spectra (270−220 K) of a complex of (R_p,*S*)-**5** and diethylzinc at a 2:1 ratio (data not shown). In this temperature range significant line broadening of any signal of (ZnEt·**5**) is not observed, indicating the absence of dynamic processes within the ligand. In general, conformations ZnEt·**5b** and ZnEt·**5d** can be considered improbable due to energetical discrimination. Because of steric reasons conformation ZnEt·**5c** with the side chain flipped away from the zinc core seems to be favored in comparison to ZnEt·**5a**.[19] All these considerations designate configuration ZnEt·**5c** being the most probable structure in solution. However, these were not underpinned by NMR experiments for paracyclophane zinc complexes with aggregation levels higher than dimers. In a NOESY spectrum of a 1:1 complex of (R_p,*S*)-**5** and diethylzinc at 260 K, the diethyl substituent shows the

(15) For example a ladder structure that has been principally postulated for methylzinc alkoxide clusters by DFT calculations: Steudel, R.; Steudel, Y. *J. Phys. Chem. A* **2006**, *110*, 8912–8924.
(16) (a) Schober, K.; Zhang, H.; Gschwind, R. M. *J. Am. Chem. Soc.* **2008**, *130*, 12310–12317. (b) Zhang, H. Structure Elucidation of Copper-Phosphoramidite Complexes in Solution. Ph.D. Thesis; University of Regensburg: Regensberg, Germany, 2007.
(17) (a) Xie, X.; Auel, C.; Heinze, W.; Gschwind, R. M. *J. Am. Chem. Soc.* **2003**, *125*, 1595–1601. (b) Henze, W.; Vyater, A.; Krause, N.; Gschwind, R. M. *J. Am. Chem. Soc.* **2005**, *127*, 17335–17342. (c) Zuccaccia, D.; Macchioni, A. *Organometallics* **2005**, *24*, 3476–3486.
(18) (a) Zhang, H.; Gschwind, R. M. *Chem.—Eur. J.* **2007**, *13*, 6691–6700. (b) Schober, K.; Hartmann, E.; Zhang, H.; Gschwind, R. M. *Angew. Chem.* **2010**, *122*, 2855–2859. *Angew. Chem., Int. Ed.*, **2010**, *49*, 2794−2797.
(19) Since the internal hydrogen bond of the free ligand can be exchanged by the zinc moiety, it can be imagined that conformation **5c** is favored in comparison to **5a**. The conformation **5c** is favored by the free (R_p,*S*)-ligand, which was shown by DFT-calculations recently: Warnke, I.; Ay, S.; Bräse, S.; Furche, F. *J. Phys. Chem. A* **2009**, *113*, 6987–6993.

Scheme 3. Formation of the Complex Resulting from (S_p,*R*)-**5** and Dimethylzinc[a]

[a] The NOE pattern hints for the shown conformation. The color of the arrows corresponds to the intensity of the cross peaks (red: very strong, blue: strong, green: weak).

strongest NOE cross peaks to one proton in the unsubstituted paracyclophane ring, followed by the interaction with the aromatic protons of the phenylethyl moiety (for the NOE network see Scheme 2b). These observations verify clearly the conformation ZnEt·**5a** as most probable in solution. The other weak NOE interactions are in agreement with this model (see SI).[20]

The reaction of Me_2Zn with (S_p,*R*)-**5** results in the formation of the complex (ZnMe·**5**), which was isolated and analyzed by NMR (Scheme 3). A complex of a 1:1 stoichiometry was identified as the sole product.[21] Surprisingly, a slightly different NOE pattern was observed in comparison to the diethylzinc complex ZnEt·**5** (for details see SI). The NOESY spectrum shows that the methyl substituent bound to zinc has a strong cross peak to the unsubstituted paracyclophane ring, which indicates that the zinc moiety is oriented downward. However, the strongest cross peak can be assigned to the methyl substituent (bound to zinc) and the methyl group of the phenylethyl side chain. This is in contrast to the conformation of ZnEt·**5**. This interaction can only arise from the conformation ZnMe·**5c**, where the side chain is flipped away from the paracyclophane.

Fortunately, it was possible to isolate suitable crystals for X-ray analysis of ZnMe·(S_p,*R*)-**5**. The corresponding structure is presented in Figure 5 and marks the first X-ray structure for a zinc complex with a [2.2]paracyclophane ligand. It can be reasoned that in the solid state a dimeric structure is present. Because enantiomeric pure (S_p,*R*)-ligand was used for this complex, only homodimers having a C_2-symmetry can be formed. The absolute configuration was confirmed crystallographically by refinement of Flack's *x*-parameter (x = 0.030(11)).[22] Both monomeric units are connected *via* a Zn_2O_2-ring system. Because of the bulky [2.2]paracyclophane ligands, the connecting entity is distorted from planarity. Usually, methyl zinc complexes with less bulky ligands possess planar ring systems.[23] Moreover, the methyl group directly connected to zinc is pushed into the [2.2]paracyclophane plane. This verifies conformation ZnMe·(S_p,*R*)-**5c** as the favored one in the solid state and in solution, in which the phenylethyl-moiety is flipped away from this plane due to steric reasons.

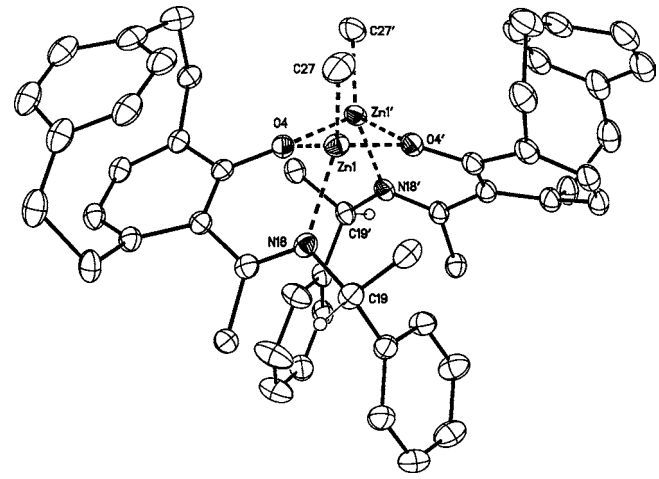

Figure 5. Molecular structure of the methylzinc complex (ZnMe·(S_p,*R*)-**5**)$_2$. (Displacement parameters are drawn at 30% probability level; solvent toluene and hydrogen atoms, except H19, H19′, are omitted for clarity.)

The combination of NLE, NMR, and X-ray studies now allows an insight into the aggregation and conformation trends of paracyclophane zinc complexes. Despite the high steric hindrance of the paracyclophane ligands, all studies consistently show aggregation of the RZnL units, mediated by the zinc moieties, and conformations with the zinc atoms pushed into the paracyclophane half-space. However, the actual level of aggregation and the conformation of the phenylethyl side chain seem to be sensitive to the individual ligand structure and the zinc reagents applied. For (R_p,*S*)-**4** and (S_p,*S*)-**4** in combination with Et_2Zn and for ZnMe·(S_p,*R*)-**5** dimeric structures were found in solution and in the solid state, whereas ZnEt·(R_p,*S*)-**5** shows aggregation numbers between 3 and 4. In agreement with the deviating aggregation level of ZnEt·(R_p,*S*)-**5** and ZnMe·(S_p,*R*)-**5,** the ligands in the two complexes adopt the different phenylethyl conformations **5a** and **5c**, respectively.

Quantum chemical calculations mainly based on density functional theory (DFT) were performed to obtain the relative energies of several dimers and monomers of ZnMe·**5** using the program package TURBOMOLE.[24] The details of the calculations are given in the paragraph "Quantum chemical calculations" in the SI. The results are summarized in Table 2; enantiomers are listed only once. We compare DFT results obtained with different exchange correlation functionals, and consider the influence of van der Waals (vdW) effects by the DFT-D method[25] and solvent effects by the COSMO method.[26]

In all calculations for the monomers, the (S_p,*R*) monomer (used in the experiment above) was about 4 kcal/mol more stable than the (S_p,*S*) isomer. The relative energies of the dimers reflect the energy differences of the monomers, the S_p,*R*/S_p,*R* dimer has the lowest and the S_p,*S*/S_p,*S* dimer the highest energy. The results of the DFT calculations are comparable for different exchange correlation functionals. For the dimers, the energy differences were increased, when van der Waals (vdW) interactions were considered by the DFT-D method.[27]

An important question was, whether the catalyst is more stable in its monomeric or dimeric form. Therefore, the dimer binding

(20) For a detailed discussions of X-Ray structures *vs* NMR structures: (a) John, M.; Auel, C.; Behrens, C.; Marsch, M.; Harms, K.; Bosold, F.; Gschwind, R. M.; Rajamohanan, P. R.; Boche, G. *Chem.—Eur. J.* **2000**, *6*, 3060–3068. (b) Xie, X.; Auel, C.; Henze, W.; Gschwind, R. M. *J. Am. Chem. Soc.* **2003**, *125*, 1595–1601. (c) For copper-complexes: Schober, K.; Zhang, H.; Gschwind, R. M. *J. Am. Chem. Soc.* **2008**, *130*, 12310–12317.

(21) The aggregation of this complex in solution was not investigated by DOSY. This material was used for X-ray analysis.

(22) Flack, H. D. *Acta Crystallogr.* **1983**, *A39*, 876–881.

(23) (a) Meyer, N.; Löhnwitz, K.; Zulys, A.; Roesky, P. W.; Dochnahl, M.; Blechert, S. *Organometallics* **2006**, *25*, 3730–3734. (b) Birch, S. J.; Boss, S. R.; Cole, S. C.; Coles, M. P.; Haigh, R.; Hitchcock, P. B.; Wheatley, A. E. H. *Dalton Trans.* **2004**, 3568–3574.

(24) *TURBOMOLE*, version 6.0; TURBOMOLE GmbH: Karlsruhe, Germany, 2008, www.turbomole.com.

(25) (a) Grimme, S. *J. Comput. Chem.* **2004**, *25*, 1463–1473. (b) Grimme, S. *J. Comput. Chem.* **2006**, *27*, 1787–1799.

(26) Klamt, A.; Schuerman, G. *J. Chem. Soc., Perkin Trans.* **1993**, *2*, 799–805.

(27) Hättig, C.; Weigend, F. *J. Chem. Phys.* **2000**, *113*, 5154–5161.

Table 2. Relative Energies of Monomers and Dimers of ZnMe·**5**, Dimer Binding Energies (in kcal/mol) for Various Diastereomers of ZnMe·**5**[a]

relative energies of the different isomers (in kcal/mol)[b]				
monomers	BP86	BP86/COSMO	B3-LYP	BP86/DFT-D
S_p,*R*	0.00	0.00	0.00	0.00
S_p,*S*	3.75	3.96	3.93	3.94
dimers	BP86	BP86/COSMO	B3-LYP	BP86/DFT-D
S_p,*R*/S_p,*R*	0.00	0.00	0.00	0.00
S_p,*R*/S_p,*S*	1.72	1.55	1.62	5.44
S_p,*S*/S_p,*S*	3.81	3.82	3.76	9.21
S_p,*S*/R_p,*R*	2.80	2.66	2.78	4.13
S_p,*S*/R_p,*S*	1.94	1.89	1.90	3.72
S_p,*R*/R_p,*S*	1.23	1.19	1.22	2.33

binding energies of the dimers (in kcal/mol)[b]				
isomer	BP86	BP86/COSMO	B3-LYP	BP86/DFT-D
S_p,*R*/S_p,*R*	2.84	4.92	0.27	−25.54
S_p,*R*/S_p,*S*	0.86	2.77	−1.76	−25.94
S_p,*S*/S_p,*S*	−0.93	0.94	−3.72	−26.24
S_p,*S*/R_p,*R*	−1.76	0.77	−5.32	−25.94
S_p,*S*/R_p,*S*	−0.39	1.96	−4.41	−25.71
S_p,*R*/R_p,*S*	−0.40	1.88	−4.83	−25.57

[a] All values were obtained with a def2-TZVP basis set. All values given include the ZPE corrections. The binding energies are corrected for the basis set superposition error. [b] $E_{bind} = E_{AB} - E_A - E_B - zpe_A - zpe_B + zpe_{AB}$ (zpe = zero-point energy; E_{AB} includes the counterpoise correction).

energies calculated by different methods are summarized in the last part of Table 2. As long as vdW interactions were not taken into account, the energies of monomers and dimers were similar. Inclusion of solvent effects (COSMO) stabilized all monomers by 2 kcal/mol. By changing the functional to B3-LYP, the dimers were slightly stabilized. When vdW interactions were considered by the DFT-D method, the dimers were strongly stabilized by about 25 kcal/mol. The strong influence of dynamic correlation was confirmed by RI-MP2 calculations for the binding energy of the (S_p,*R*) homodimer. For this isomer the total binding energy amounts to −32.9 kcal/mol at MP2 level.

In the following, we focus our discussion on the homodimer and heterodimer formed by the (S_p,*R*) and (R_p,*S*) monomers. The calculated values show that the homodimers are around 2 kcal/mol more stable than the heterodimer. However, such a stabilization is very small and prompted us to investigate which factors affect the relative stability of the dimers. To gain insight into the thermochemistry of the dimer formation the zero-point energies were obtained from the frequency calculations and are already included in the binding energies given in Table 2. The change in standard internal energy at 0 K ($\Delta U^o(0) = zpe_{dimer} - \Sigma_{monomer,i}\ zpe_i$) equals 1.3 kcal/mol for the homodimer and 6.1 kcal/mol for the heterodimer. At the reaction temperature of 248 K the homodimer has an entropic stabilization of 4.2 kcal/mol compared to that of the heterodimer. While the reaction proceeds in a nonpolar medium, the greater size of the polar surface of one dimer will cause its destabilization in this solvent. Topological molecular polar surface area[28] (TPSA) calculations give a value of 25 Å^2 for the homodimer, while the value for the heterodimer amounts to 33 Å^2. A simple explanation of these results is that the polar center of the homodimer is better shielded. Moreover, the considered molecules contain several phenyl rings which can interact with the toluene molecules. This interaction is not included in the COSMO model, but can be estimated in the following way. According to the work of Sinnokrot and Sherrill[29] the $\pi-\pi$ sandwich interaction is in the order of −2.3 kcal/mol at an optimal distance of 3.8 Å. Both dimers can at least interact with six toluene molecules, each phenyl ring with one solvent molecule. In contrast to the heterodimer, the homodimer possesses an extra pocket between the two phenyl rings in the side chain. The distance between them is around 7.5 Å so that there is a place for at least one additional toluene ring. This extra stabilization has been estimated on the basis of a small model system containing two benzene rings and a toluene molecule in the middle. A binding energy of −7.3 kcal/mol was obtained at DFT-D level (BP86, def2-TZVP basis set).

In summary, the calculations confirm the experimental finding that the catalyst is mainly in its dimeric form. However, in solution, the stabilization of the dimers will be less pronounced, because of dispersion interactions of the monomer with solvent molecules, which can fill the space occupied by the second molecule in the dimer. The (S_p,*R*) homodimer has been found to be the most stable dimer and is favored mainly by entropy contributions and solvent interaction.

3. Conclusions

In this study first indications were found to understand the cometal-free asymmetric 1,4-selectivity of paracyclophane ligands in the addition of dialkylzinc to enals. In accordance to the well-established ML_2-systems found for similar Zn-catalyzed reactions using bidentate ligands such as DAIB, NMR studies of paracyclophane zinc complexes including DOSY investigations and the first X-ray structure of a zinc complex with a [2.2]paracyclophane ligand show consistently the existence of $(ZnL)_n$ complexes. The observed negative NLE and the X-ray analysis as well as the theoretical studies are in agreement with the formation of dimeric species $(ZnL)_2$ that serve as precatalysts.

In addition, the NLE investigations of mixtures of diastereomeric catalysts indicate the existence of additional possible aggregates, which are very likely oligomeric $(ZnL)_n$ complexes as found in the DOSY investigations of very similar complexes. The presented results from NLE, NMR, and X-ray investigations show that the level of aggregation *n* in these $(ZnL)_n$ complexes is very sensitive to temperature and concentration.

As a proposal resulting from the presented investigations, the 1,4-selectivity of these complexes may be caused by the $(ZnL)_2$ structure of the paracyclophane zinc complexes, which allows cooperative clusters as found in the 1,4-addition reactions of organocuprates or just enlarges the distance between coordinating Zn and the transferable alkyl moiety.

4. Experimental Section

Crystal Structure Study of (ZnMe·5)$_2$. The single-crystal X-ray diffraction study of (ZnMe·**5**)$_2$ was carried out on a Bruker-Nonius APEXII diffractometer at 123(2) K using Mo K_α radiation (λ = 0.71073 Å). Direct methods (SHELXS-97)[30] were used for structure solution, and refinement was carried out using SHELXL-97 (full-matrix least-squares refinement on F^2).[30] H atoms were localized by difference Fourier synthesis and refined using a riding model. A semiempirical absorption correction was applied (max/min

(28) Ertl, P.; Rohde, B.; Selzer, P. *J. Med. Chem.* **2000**, *43*, 3714–3717.
(29) Sinnokrot, M. O.; Sherrill, C. D. *J. Am. Chem. Soc.* **2004**, *126*, 7690–7697.
(30) Sheldrick, G. M. *Acta Crystallogr.* **2008**, *A64*, 112–122.

transmission 0.8799/0.7515). The absolute configuration was confirmed by refinement of Flack's *x*-parameter ($x = 0.030(11)$).[22]

$(ZnMe\cdot\mathbf{5})_2$: yellow crystals, $C_{54}H_{58}N_2O_2Zn_2 - 0.5$ toluene, $M = 943.83$, crystal size 0.35 mm × 0.20 mm × 0.15 mm, trigonal, space group $P3_121$ (No. 152): $a = 13.2807(4)$ Å, $c = 52.5695(17)$ Å, $V = 8029.8(4)$ Å^3, $Z = 6$, ρ(calcd) = 1.171 Mg m^{-3}, $F(000) = 2982$, $\mu = 0.936$ mm^{-1}, 88125 reflections ($2\theta_{max} = 55°$), 12234 unique [$R_{int} = 0.069$], 599 parameters, 84 restraints, R1 ($I > 2\sigma(I)$) = 0.046, wR2 (*all data*) = 0.120, GooF = 1.09, largest diff. peak and hole 0.509 and −0.390 e·Å^{-3}.

Crystallographic data (excluding structure factors) for the structure reported in this work have been deposited with the Cambridge Crystallographic Data Centre as supplementary publication no. CCDC-723473 ($(ZnMe\cdot\mathbf{5})_2$). Copies of the data can be obtained free of charge on application to The Director, CCDC, 12 Union Road, Cambridge DB2 1EZ, U.K. (Fax: int.code +(1223) 336-033; E-mail: deposit@ccdc.cam.ac.uk).

Acknowledgment. This work has been supported by the *Fonds der Chemischen Industrie* (fellowship for S.A.). K.F. was supported by the *Deutsche Forschungsgemeinschaft* (DFG) through the Center for Functional Nanostructures (CFN) in Karlsruhe.

Supporting Information Available: Time-dependence of the product *ee*, mathematical models used for the fitted curves of the NLE diagrams, NMR spectroscopy, NMR characterization of the complexes and quantum chemical calculations; crystallographic file in CIF format. This material is available free of charge *via* the Internet at http://pubs.acs.org.

JA1032502